Dieses Dokument ist eine Zweitveröffentlichung (Verlagsversion) /

This is a self-archiving document (published version):

Nicholas S. Colella, Lei Zhang, Thomas McCarthy-Ward, Stefan C. B. Mannsfeld, H. Henning Winter, Martin Heeney, James J. Watkins, Alejandro L. Briseno

Controlled integration of oligo- and polythiophenes at the molecular scale

Diese Version ist verfügbar / This version is available on:

https://nbn-resolving.org/urn:nbn:de:bsz:14-qucosa2-363733

SLUB
Wir führen Wissen.

TECHNISCHE UNIVERSITÄT DRESDEN

Qucosa
Quality Content of Saxony

Controlled integration of oligo- and polythiophenes at the molecular scale†

Nicholas S. Colella,[a] Lei Zhang,[a] Thomas McCarthy-Ward,[b] Stefan C. B. Mannsfeld,[cd] H. Henning Winter,[a] Martin Heeney,[b] James J. Watkins*[a] and Alejandro L. Briseno*[a]

High molecular weight PBTTT-C_{12} is blended with the pure trimer, BTTT-3, to enhance intergrain connectivity and charge transport. Analysis of the morphology and crystallinity of the blends shows that the polymer and oligomer are well-integrated, leading to high hole mobilities, greater than 0.1 cm^2 V^{-1} s^{-1}, in films that contain as much as 83% oligomer.

The past decade has seen an explosion in the growth of polymer-based organic electronics. Organic photovoltaics (OPVs) and field-effect transistors (OFETs) have reached record efficiencies and mobilities, respectively, and their further development will continue to enhance their performance.[1–4] Most needed is a fundamental understanding of morphological control.[5] In particular, the effect of one product of virtually every polymerization, low molecular weight oligomers, is often neglected or even discarded.[6,7] These low molecular weight components have been considered impurities or trapping sites and, while there have been some recent efforts to characterize pure oligomers, the role of a pure, well-defined oligomer component in polymer thin films has not been thoroughly studied.[8–12]

Electronic properties of organic semiconductor thin films are heavily dependent on their morphology.[13,14] Small molecules typically exhibit a higher degree of crystallinity, producing large grains, with poor electronic communication between the grains due to the large grain boundaries. While charge transport within the crystallites is rapid, as shown in single-crystal devices,[15] the lack of continuity in low molecular weight films deposited *via* typical solution methods (*e.g.* spin coating) leads to generally low measured mobilities in thin film transistors. In contrast, high molecular weight polymers generally produce relatively uniform films with small crystallites that are well-connected *via* long polymer "tie chains" in the amorphous regions.[13]

Poly(2,5-bis(3-alkylthiophen-2-yl)thieno[3,2-*b*]thiophene) (PBTTT-C_{12}) is an excellent model polymer semiconductor, as it displays relatively high crystallinity due to intermolecular interactions between neighboring chains, both through π–π stacking between backbones and side chain interactions.[16,17] We have previously synthesized and characterized thiophene oligomers and determined that the trimer, BTTT-3, is an excellent model oligomer for this family of molecules. The monomer, BTTT-1, packs in a two dimensional (2-D) motif, characteristic of small molecules, and the dimer, BTTT-2, shows significant misorientation with respect to the substrate (Fig. S1, ESI†). In contrast, BTTT-3 exhibits a well-defined lamellar packing, and is therefore the shortest macro-molecule that is representative of the polymer.

In this work we report the morphological and electronic properties of blended films consisting of BTTT-3 and PBTTT (Fig. 1) in different ratios in order to characterize the interplay between crystallinity, connectivity, and charge transport. The combination of enhanced crystallinity of low-molecular weight oligomers, due to their lower entropic frustration, with the inter-grain connectivity afforded by polymeric PBTTT is characterized and the relationship between the resulting morphology and device performance is analyzed. The results show that the oligomer and polymer are well-integrated on the molecular level and that high charge mobility can be achieved in films that contain a majority of low molecular weight oligomer.

The oligomer BTTT-3 was synthesized as previously reported *via* Stille coupling, with a molecular weight of 1917 g mol^{-1} as
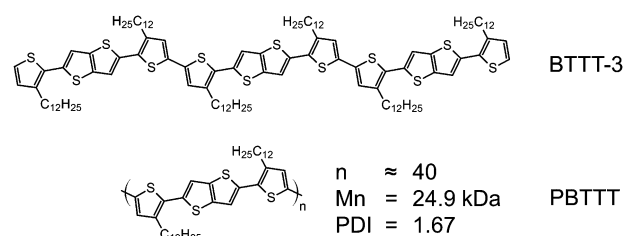
[a] *Department of Polymer Science and Engineering, Conte Research Center, University of Massachusetts, 120 Governors Drive, Amherst, MA, 01002, USA. E-mail: watkins@polysci.umass.edu, abriseno@mail.pse.umass.edu*

[b] *Department of Chemistry, Imperial College London, London, SW7 2AZ, UK*

[c] *Dresden University of Technology, Center for Advancing Electronics Dresden, 01062 Dresden, Germany*

[d] *Stanford Synchrotron Radiation Lightsource, Menlo Park, CA, 94025, USA*

† Electronic supplementary information (ESI) available. See DOI: 10.1039/c4cp02944e

Fig. 1 Molecular structures of the oligomer, BTTT-3, and polymer, PBTTT, used in this study.

This journal is © the Owner Societies 2015

Phys. Chem. Chem. Phys., 2015, **17**, 26525–26529 | **26525**

measured by matrix-assisted laser desorption/ionization time-of-flight (MALDI-TOF) using a Bruker MicroFlex. The PBTTT used in this study was synthesized according to the literature and was characterized by gel-permeation chromatography (GPC) using an Agilent PL-GPC 220, which showed a number-average molecular weight of 24.9 kg mol^{-1} with a dispersity of 1.67 against polystyrene (PS) standards.[16] It is important to note that, owing to the relatively rigid nature of PBTTT, as opposed to the flexible PS standard, this molecular weight is likely an overestimation, as the GPC of BTTT-3 produced a number-average molecular weight of 3337, 74% higher than that observed *via* MALDI-TOF. All films were spun-cast at 2000 RPM for 1 minute from a 2 mg mL^{-1} solution in hot chlorobenzene and were characterized as-spun on SiO$_2$ (diffraction was done on films spun onto native silicon).

The atomic force microscopy (AFM) images, obtained with a Veeco Dimension 3100 in tapping mode, in Fig. 2 showed ∼50–100 nm crystallites in the pure BTTT-3 film. As seen in Fig. 2b, the addition of a small amount of polymer (∼17% by weight) completely changed the morphology to that of a continuous film with a terraced-like structure, similar to that previously observed in annealed pure PBTTT films.[18,19] Increasing the percentage of polymer in the film to 50% generated a nodule-like structure that is typical of polymer semiconductor thin films, and the further addition of polymer did not significantly change the surface morphology. These results demonstrated that any polymer present in the systems dominated the surface morphology and significantly enhanced the connectivity of the films.

In probing the microstructure of the thin films *via* grazing-incidence wide-angle X-ray scattering (GIWAXS), there was a striking contrast between the pure oligomer thin films and the films that contained a nominal amount of polymer (Fig. 3). In all films, the molecules adopted an edge-on orientation as demonstrated by the Q_{xy} peaks at ∼1.7 Å^{-1}, which correspond
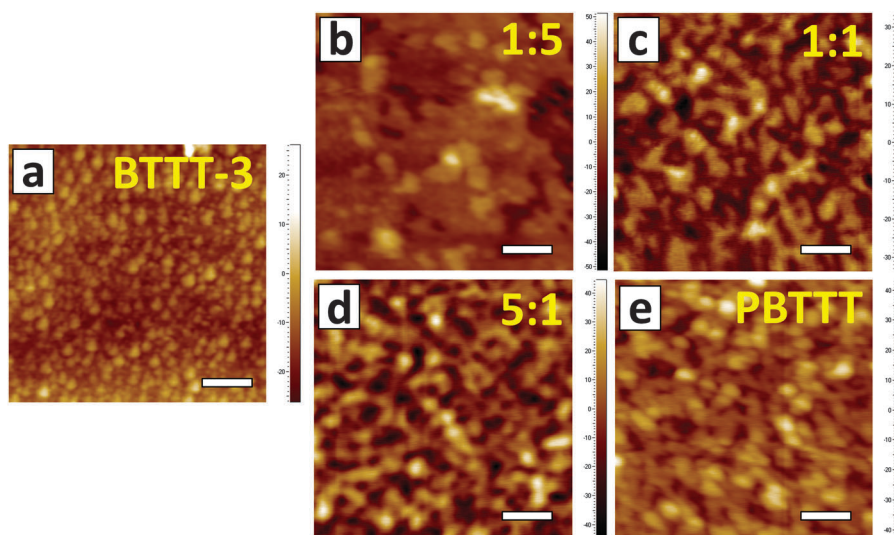

Fig. 2 Atomic force micrographs: surface height of (a) 100% BTTT-3, (b) 87% BTTT-3/13% PBTTT, (c) 50% BTTT-3/50% PBTTT, (d) 13% BTTT-3/87% PBTTT, and (e) 100% PBTTT thin films. Scale bar is 200 nm. Vertical scale is in Å.
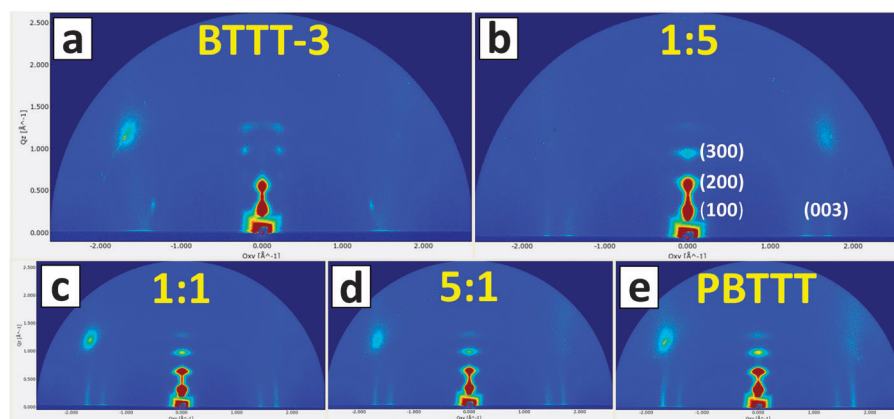

Fig. 3 Grazing-incidence wide-angle X-ray scattering (GIWAXS) diffractograms of (a) 100% BTTT-3, (b) 87% BTTT-3/13% PBTTT, (c) 50% BTTT-3/50% PBTTT, (d) 13% BTTT-3/87% PBTTT, and (e) 100% PBTTT thin films. The Q_{xy} value of the peaks for the pure BTTT-3 film corresponds to 3 nm, indicating that the oligomer is fully extended in its crystal packing. In the films that contain a nominal amount of polymer, the diffraction is virtually identical to the pure polymer film.

26526 | *Phys. Chem. Chem. Phys.*, 2015, **17**, 26525–26529

This journal is © the Owner Societies 2015

to the π–π stacking distance of $\sim$3.7 Å. While we were unable to obtain a complete crystal structure of the trimer from single-crystal X-ray scattering, the single crystal unit cell parameters of BTTT-3 were determined to be a = 9.9 Å, b = 12.4 Å, c = 22.3 Å, and α = 92°, β = 102°, γ = 100.7°. The Q_z peaks observed in the GIWAXS diffractograms from the thin films correspond well with the c axis of the single crystal unit cell, which is the direction of side chain packing. However, the clearly visible Bragg rods at Q_{xy} = 0.2 Å^{-1} in the thin film BTTT-3 diffraction image are not compatible with the a–b plane of the single crystal cell, and, while there are faint higher orders of this single rod at 0.2 Å^{-1}, not a single peak was found that could be attributed to the single crystal cell (besides the lamellar stacking peaks). It is therefore safe to conclude that BTTT-3 forms a thin film phase on silicon that significantly differs from the single crystal packing. The in-plane value of at Q_{xy} = 0.2 Å^{-1} corresponds to a repeat length of $\sim$3 nm which incidentally is quite close to the length of a BTTT-3 aromatic backbone. This suggests in this thin film phase one lattice vector more or less spans the pi–pi stacking direction while the other one is along the long axis of the fully extended oligomer backbone as schematically shown in Fig. 4. Due to the great length of the oligomer (in comparison with the monomer or other small molecules), there is little energetic driving force for phase separation between oligomers and polymer molecules, and the polymer seems to integrate seamlessly

into the BTTT-3 crystallites for all blends. The incorporation of the polymer into oligomer domains as schematically shown in the cartoon Fig. 4 is consistent with the disappearance of the Bragg rods with a nominal amount of polymer (Fig. 3b). When a sufficient amount of polymer chains gets embedded in the oligomer domains, the spatial coherence especially along the lattice axis along the long oligomer axis becomes severely disturbed, eventually leading to the disappearance of the 0.2 Å^{-1} peak above a certain threshold polymer load. In the present case, a 13% PBTTT loading is already enough to quench the in-plane peak from the 3 nm repeat length (0.2 Å^{-1}). The pi–pi stacking peak on the other hand is unaffected by this since the polymer will incorporate at the same pi–pi spacing in the lattice as the pure oligomers.

A TA Instruments Q1000 differential scanning calorimeter (DSC) was also used to examine the crystallinity of the blends (Fig. 5). The samples were prepared by drop-casting the material directly into the DSC pans. The DSC data contained herein was obtained during the second heating cycle to erase the thermal history of the material and the heating rates were 1 K min^{-1} and 5 K min^{-1} for the BTTT-3 and PBTTT melting regions, respectively, to obtain clear endotherms. In the pure oligomer sample, two melting points were observed owing to the liquid crystalline nature of BTTT. In BTTT-3, the melting of the alkyl side chains was observed at $\sim$62 °C, while the backbone melted at 95 °C.

Fig. 4 Illustration of the proposed mixing of BTTT-3 and PBTTT chains within crystallites.
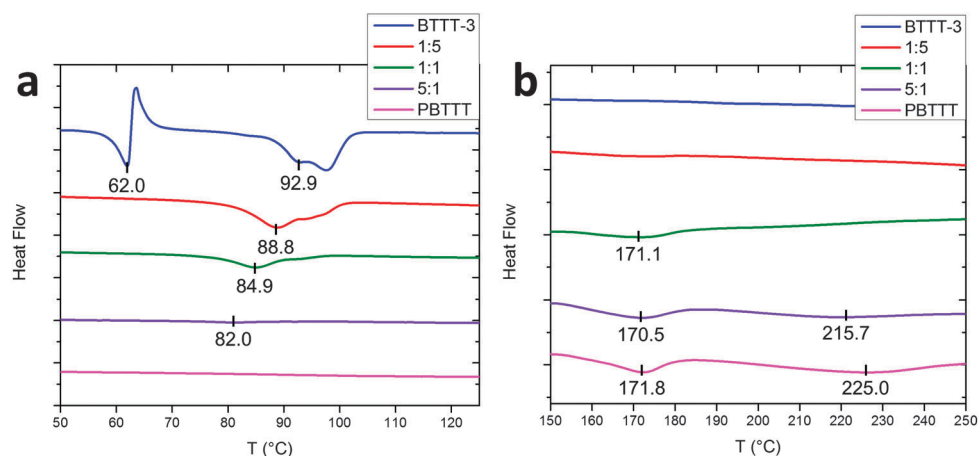

Fig. 5 Differential scanning calorimetry traces for the side chain and backbone melting regions of (a) BTTT-3 and (b) PBTTT (endo down). Note the absence of the BTTT-3 side chain melting at 62.0 °C for all blends that contain PBTTT. The depressed melting points for the BTTT-3 and PBTTT backbones from 92.9 °C to 82.0 °C and 225.0 °C to 215.7 °C, respectively, indicated that the crystallites were less pure.
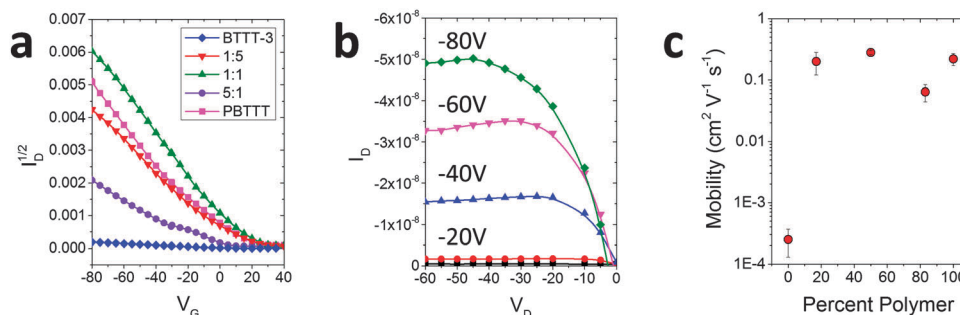
Fig. 6 Characteristics for polymer/oligomer blend OFETS (a) Square root of transfer curves. $V_{DS} = -60$ V (b) characteristic output curve for the 5 : 1 blend. Gate voltages are noted in the figure. (c) Graph of mobilities *vs.* percent of polymer in blend composition.

The apparent melting of BTTT-3 side chains was notably absent for all blended films, and alkyl side chain melting was only observed at ~171 °C, which is characteristic of PBTTT. The melting point for the BTTT-3 backbones was depressed for the blended systems, indicating that the crystallites were decreasing in size and purity as the amount of polymer present was increased. Additionally, the backbone melting temperature of PBTTT, *ca.* 225 °C, was depressed upon the addition of a minimal amount of BTTT-3. These results suggest that the polymer and oligomer formed an intimate phase on the molecular level.

In order to characterize the electronic properties of these blended films, field-effect transistors were fabricated. All electrical measurements were performed in ambient conditions using a standard probe station connected to a Keithley 4200-SCS Parameter Analyzer, and the thin film transistors were fabricated using a bottom gate, bottom contact geometry on lithographically patterned substrates. The OFET measurements exactly mirrored the changes observed in the morphology (Fig. 6) (Table 1). Devices fabricated from the pure oligomer exhibited low mobilities of ~10^{-4} cm^2 V^{-1} s^{-1} due to the large grain boundaries. The crystal domains observed *via* AFM had limited interconnectivity which led to poor charge transport across the films. However, the films that contained up to 83% oligomer exhibited mobilities equal to or even surpassing those of the neat polymer film. The enhanced crystallinity from the BTTT-3 also led to slightly higher mobilities in the 50% blend. One can observe a slight decrease in the 13% oligomer blend, which we attributed to oligomer chains passivating PBTTT crystals, reducing the number of tie chains while also not contributing any increased crystallinity, as observed by the lack of BTTT-3 melting peak in the DSC trace.

These results demonstrate that oligomers are not "impurities," as they are often construed. Their enhanced crystallinity due to their lower entropic frustration can actually be beneficial for charge transport as observed in the 50% blend. This serves as a counterexample to the general assumption that oligomers act as charge trapping sites. This idea may arise from the common observation that semiconducting polymers which have been purified *via* Soxhlet extraction generally exhibit better performance than those which have not. The results shown here suggest that it may be beneficial to selectively incorporate significant amounts of pure oligomer extracted from the lower molecular weight fraction back into the final composition to enhance the crystallinity within thin films. This strategy could be applied to fabricate devices with higher performance while maximizing the use of all polymerization products.

Acknowledgements

References

1 J. You, L. Dou, K. Yoshimura, T. Kato, K. Ohya, T. Moriarty, K. Emery, C.-C. Chen, J. Gao, G. Li and Y. Yang, *Nat. Commun.*, 2013, **4**, 1446.

2 Z. He, C. Zhong, S. Su, M. Xu, H. Wu and Y. Cao, *Nat. Photonics*, 2012, **6**, 593–597.

3 H.-R. Tseng, H. Phan, C. Luo, M. Wang, L. A. Perez, S. N. Patel, L. Ying, E. J. Kramer, T.-Q. Nguyen, G. C. Bazan and A. J. Heeger, *Adv. Mater.*, 2014, **26**, 2993–2998.

4 J. Mei, Y. Diao, A. L. Appleton, L. Fang and Z. Bao, *J. Am. Chem. Soc.*, 2013, **135**, 6724–6746.

5 J. Rivnay, S. C. B. Mannsfeld, C. E. Miller, A. Salleo and M. F. Toney, *Chem. Rev.*, 2012, **112**, 5488–5519.

6 R. J. Kline, M. D. McGehee, E. N. Kadnikova, J. Liu and J. M. J. Fréchet, *Adv. Mater.*, 2003, **15**, 1519–1522.

Table 1 Summary of device characteristics for all blends

Sample	Mobility (cm^2 V^{-1} s^{-1})	$V_{Threshold}$ (V)	$I_{On/Off}$
BTTT-3	$2.5 \pm 1.3 \times 10^{-4}$	-2.9 ± 10.9	10^3
1 : 5	$2.0 \pm 0.8 \times 10^{-1}$	5.4 ± 10.3	10^3–10^4
1 : 1	$2.8 \pm 0.2 \times 10^{-1}$	10.8 ± 4.8	10^3–10^4
5 : 1	$6.4 \pm 2.0 \times 10^{-2}$	5.7 ± 9.9	10^3
PBTTT	$2.2 \pm 0.5 \times 10^{-1}$	0.8 ± 1	10^3–10^4

26528 | *Phys. Chem. Chem. Phys.*, 2015, **17**, 26525–26529

This journal is © the Owner Societies 2015

7 S. Joshi, S. Grigorian, U. Pietsch, P. Pingel, A. Zen, D. Neher and U. Scherf, *Macromolecules*, 2008, **41**, 6800–6808.

8 L. Zhang, N. S. Colella, F. Liu, S. Trahan, J. K. Baral, H. H. Winter, S. C. B. Mannsfeld and A. L. Briseno, *J. Am. Chem. Soc.*, 2013, **135**, 844–854.

9 P. Bäuerle and J. Cremer, *Chem. Mater.*, 2008, **20**, 2696–2703.

10 A. R. Murphy and J. M. J. Fréchet, *Chem. Rev.*, 2007, **107**, 1066–1096.

11 M. Banerjee, R. Shukla and R. Rathore, *J. Am. Chem. Soc.*, 2009, **131**, 1780–1786.

12 L. Zhang, N. S. Colella, B. P. Cherniawski, S. C. B. Mannsfeld and A. L. Briseno, *ACS Appl. Mater. Interfaces*, 2014, **6**, 5327–5343.

13 R. Noriega, J. Rivnay, K. Vandewal, F. P. V Koch, N. Stingelin, P. Smith, M. F. Toney and A. Salleo, *Nat. Mater.*, 2013, **12**, 1038–1044.

14 J. A. Lim, F. Liu, S. Ferdous, M. Muthukumar and A. L. Briseno, *Mater. Today*, 2010, **13**, 14–24.

15 V. Podzorov, *MRS Bull.*, 2013, **38**, 15–24.

16 I. McCulloch, M. Heeney, C. Bailey, K. Genevicius, I. Macdonald, M. Shkunov, D. Sparrowe, S. Tierney, R. Wagner, W. Zhang, M. L. Chabinyc, R. J. Kline, M. D. McGehee and M. F. Toney, *Nat. Mater.*, 2006, **5**, 328–333.

17 T. Schuettfort, B. Watts, L. Thomsen, M. Lee, H. Sirringhaus and C. R. McNeill, *ACS Nano*, 2012, **6**, 1849–1864.

18 R. J. Kline, D. M. DeLongchamp, D. A. Fischer, E. K. Lin, L. J. Richter, M. L. Chabinyc, M. F. Toney, M. Heeney and I. McCulloch, *Macromolecules*, 2007, **40**, 7960–7965.

19 A. Gasperini and K. Sivula, *Macromolecules*, 2013, **46**, 9349–9358.